RSC Advances

COMMUNICATION

View Article Online
View Journal | View Issue

Cite this: *RSC Adv.*, 2016, **6**, 55750

Received 11th February 2016
Accepted 3rd June 2016

DOI: 10.1039/c6ra03824g

www.rsc.org/advances

Designed synthesis of well-defined titania/iron(III) acetylacetonate nanohybrids with magnetic/luminescent properties†

Kota Shiba,*[ab] Takuya Kataoka,[c] Mitsuhiro Okuda,[de] Santiago Blanco-Canosa[de] and Motohiro Tagaya*[cf]

A controlled sol–gel reaction of titanium tetraisopropoxide and Fe(III) acetylacetonate was conducted in the presence of octadecylamine by means of a microfluidic synthetic approach. This resulted in the formation of monodispersed titania/octadecylamine/Fe(III) acetylacetonate nanohybrids with spherical shape and magnetic/luminescent properties.

Titania has attracted much attention because of its physical/chemical properties that are useful for such applications as pigments, photocatalysts, and UV-shielding materials. In the past two decades, many researchers working in application development have tried to obtain titania nanomaterials for realizing novel properties based on the engineered nanostructures. Accordingly, various wet-synthetic techniques have become available, resulting in the controlled synthesis of titania-based diverse particulates toward a wider range of applications. Hetero-atom/molecule doping is known as an effective way to modify physical/chemical properties of a matrix material. Thus, this type of approaches has been applied to obtain titania with precisely modified characteristics. A number of dopants including Al,[1,2] Ga,[2] In,[2] Zr,[1,3,4] Au,[5] B,[6] Cd,[7] Cl,[8] C,[9,10] Eu,[11,12] Sm,[11] Fe,[13,14] F,[15–17] N[18,19] and Si[20] have been utilized for the modified titania synthesis. There are many examples of the titania-based particulates and their modified properties; however, the detailed physicochemical mechanism of the obtained properties is still unclear because of the technical difficulties in synthesizing ideal products for such a purpose.

To explore the mechanism, one of the important challenges is the synthesis of the heterospecies-doped titania with the well-defined sizes/shapes. These features are indispensable for the detailed and quantitative discussion on nanomaterial properties since possible effects of size, shape and/or the presence of by-products can be ignored. A problem is that the synthesis of the doped titania frequently leads to the formation of polydispersed, aggregated or phase-separated product because of the different reactivity of starting materials. A small number of successful examples have been reported on the synthesis of the doped titania with the well-defined sizes/shapes,[2–4,10,12,16,17,20] while each synthesis was conducted based on a different scheme. Therefore, the development of a general approach is demanded to prepare a variety of the doped titania more efficiently and to clarify the mechanism.

In the present study, we demonstrate the synthesis of well-defined titania/octadecylamine (ODA) hybrid particles containing iron(III) acetylacetonate ($Fe(acac)_3$) molecules (see ESI† for experimental details). Taking advantage of the interaction between the titania and acetylacetonate,[21,22] the titania and $Fe(acac)_3$ nanohybrids were formed with the molecular level homogeneity. As described, this uniform feature is very important and helped discuss the relationship between the unexpected, interesting nanomaterial properties shown later and their possible reasons/mechanisms. A microfluidic approach, which we previously reported, was successfully applied to control the sizes and shapes of the nanohybrids.[23,24] The nanohybrids exhibited paramagnetic property, which is reasonable and easy to be predicted from the presence of the iron complex. Interestingly, we also found that the nanohybrids possessed a luminescent property that would be due to the uniform distribution of $Fe(acac)_3$ in the nanohybrids.

[a]*International Center for Young Scientists (ICYS), National Institute for Materials Science (NIMS), 1-1 Namiki, Tsukuba 305-0044, Japan. E-mail: SHIBA.Kota@nims.go.jp*

[b]*World Premier International Research Center Initiative (WPI), International Center for Materials Nanoarchitectonics (MANA), National Institute for Materials Science (NIMS), 1-1 Namiki, Tsukuba, Ibaraki 305-0044, Japan*

[c]*Department of Materials Science and Technology, Nagaoka University of Technology, 1603-1 Kamitomioka, Nagaoka, Niigata 940-2188, Japan. E-mail: tagaya@mst.nagaokaut.ac.jp*

[d]*CIC nanoGUNE, Tolosa Hiribidea 76, E-20018 Donostia-San Sebastian, Basque Country, Spain*

[e]*Ikerbasque, Basque Foundation for Science, Alameda Urquijo 36-5, Plaza Bizkaia, E-48011, Bilbao, Basque Country, Spain*

[f]*Top Runner Incubation Center for Academica-Industry Fusion, Nagaoka University of Technology, 1603-1 Kamitomioka, Nagaoka, Niigata 940-2188, Japan*

† Electronic supplementary information (ESI) available: Detailed experimental method, additional Scheme S1 and Fig. S1–S9. See DOI: 10.1039/c6ra03824g

For the synthesis of well-defined nanohybrids composed of titania, ODA and $Fe(acac)_3$, labeled as titania/ODA/$Fe(acac)_3$, a sol–gel reaction of titanium tetraisopropoxide (TTIP) was conducted in a controlled environment utilizing a microfluidic approach.[23,24] The molar Fe/Ti ratio in the starting solution was set at 0.02. An image of the experimental setup is illustrated in Fig. S1.† $Fe(acac)_3$ was mixed with TTIP to obtain a clear, slightly reddish starting solution. This homogeneous solution is important for this microfluidic synthesis, being consumed to form uniform sized nuclei. According to the previous reports, the microfluidic approach leads to the separation of nucleation and growth processes, resulting in the formation of monodispersed products.[23,24] The detailed synthetic and characterization methods were described in the experimental procedures and characterization in ESI.†

As shown in Fig. 1, well-defined spherical nanohybrids were obtained through the microfluidic synthesis. The product showed a narrow particle size distribution with the average size of 195 nm and coefficient of variation (CV) of 5.5% in the case of the titania/ODA/$Fe(acac)_3$ synthesis. These values are almost the same as those of the titania/ODA nanohybrids, which were synthesized by the same approach without adding $Fe(acac)_3$. Specifically, the average size of the titania/ODA nanohybrids was 166 nm and the CV value was 5.9%. The slight difference in the size is probably due to the incorporation of $Fe(acac)_3$ molecules. We confirmed that the reaction time of around 20 h was enough to reach sample yield of higher than 90% for titania/ODA nanohybrids. In the case of the titania/ODA/$Fe(acac)_3$ nanohybrids, the reaction solution became turbid in a few tens of seconds, which is the same as that in the case of the titania/ODA nanohybrids. No precipitate with deep red color was observed after the reaction. Thus, most of the starting materials should be consumed to form the titania/ODA/$Fe(acac)_3$ nanohybrids with no segregation of the $Fe(acac)_3$.

An FT-IR spectrum of the titania/ODA/$Fe(acac)_3$ shown in Fig. S2 in ESI† revealed that the whole spectral profile was almost identical to that of the titania/ODA except for a few characteristic absorption bands. For example, a few additional absorption bands are seen at 1586 cm^{-1} together with 1529 cm^{-1} for the titania/ODA/$Fe(acac)_3$, both of which are due to the combination of ν(C–C) + ν(C–O).[21,25,26] Another band appeared at 1283 cm^{-1} can be attributed to ν(C–C),[26] supporting the presence of $Fe(acac)_3$. A center of an absorption band (700–1000 cm^{-1}), which can be assigned to a Ti–O–Ti vibrational mode, shifted from 810 cm^{-1} to 850 cm^{-1}. This is an evidence where $Fe(acac)_3$ interacts with titania. A broad absorption band at around 3000–3700 cm^{-1} is due to the presence of OH groups on oxide surface. It should be noted here that the center of this band also shifts from 3370 cm^{-1} to 3410 cm^{-1}. Taking into account that ν(C–O) of $Fe(acac)_3$ did not show a clear shift by its introduction into the nanohybrids, specific interactions such as hydrogen bonding are not present between C=O of $Fe(acac)_3$ and surface OH groups of titania. Therefore, O atoms consisting of Fe–O in $Fe(acac)_3$ would mainly induce the spectral shifts. The XRD patterns revealed that the titania/ODA/$Fe(acac)_3$ nanohybrids were amorphous (Fig. S3, ESI†), allowing to obtain the hybrid with the various Fe/Ti ratios because of their flexible Ti–O–Ti amorphous network structures.

To obtain the direct evidence for the $Fe(acac)_3$ incorporation into the present particles, the exact composition of the titania/ODA/$Fe(acac)_3$ nanohybrids were examined by spectroscopic techniques. The content of Ti, O, Fe and C atoms was quantified by an XRF analysis and the results are summarized in Fig. S1.† It should be mentioned that Fe/Ti molar ratio was 0.02 as revealed by the XRF analysis, indicating that the Fe/Ti ratio in the titania/ODA/$Fe(acac)_3$ nanohybrids was almost the same as the initial ratio between Fe from $Fe(acac)_3$ and Ti from TTIP used in the synthesis. In addition, SEM-EDS analyses were also performed to determine the composition of the products (Fig. S4, ESI†). The peak was observed at around 6.2 keV for the titania/ODA/$Fe(acac)_3$, while no peak was seen at the same position in the case of the titania/ODA. This peak can be attributed to the characteristic X-ray line of FeKα, demonstrating the presence of $Fe(acac)_3$ in the nanohybrids. Furthermore, the peak ratio of FeKα and TiKα from the titania/ODA/$Fe(acac)_3$ was 0.017. This result also indicates that the Fe/Ti ratio in the nanohybrids is almost the same as that used in the present synthesis. These XRF and SEM-EDS results suggest that this synthesis method successfully led to the formation of monodispersed nanohybrids with the same elemental ratio to that in the synthesis solution. More importantly, the $Fe(acac)_3$ molecules are distributed homogeneously in the nanohybrids as judged from the IR results (Fig. S2, ESI†) in which interactions between titania and $Fe(acac)_3$ are indicated. We have already achieved the synthesis of monodispersed titania/silica-based spherical nanohybrids and confirmed that all the elements included in the nanohybrids were distributed homogeneously by means of TEM-EDS and other techniques.[20] As the present synthesis was conducted in a similar manner, the titania/ODA/$Fe(acac)_3$ nanohybrids would have a homogeneous structure in terms of their elemental distribution. Therefore, the obtained well-defined titania/ODA/$Fe(acac)_3$ nanohybrids allow us to investigate and discuss their properties in detail.

TG-DTA results also revealed that most of the added $Fe(acac)_3$ were incorporated into the nanohybrids (Fig. S5†).

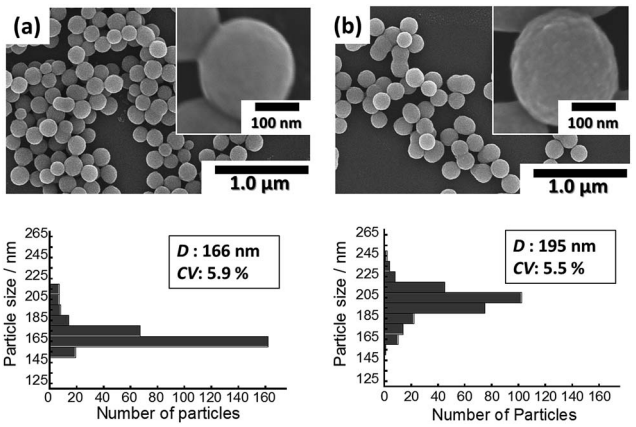

Fig. 1 FE-SEM images (inset: magnified particle images) and the particle size distributions of the (a) titania/ODA and (b) titania/ODA/$Fe(acac)_3$ nanohybrids.

Interestingly, titania/ODA/Fe(acac)$_3$ showed the first weight loss/exothermic peak at around 195 °C, which is almost 40 °C lower than that observed for titania/ODA. According to a previous study,[27] this would be due to the thermal decomposition of Fe(acac)$_3$ while ODA should also start decomposing simultaneously.[23] The thermal decomposition results in an intense exothermic reaction, which may affect crystal phase transition of titania from amorphous to other phases.

Since the titania/ODA/Fe(acac)$_3$ contains a potential magnetic element in its structure, we first measured the magnetic property of the nanohybrids. To confirm the existence of a magnetic property, a magnetic force microscope (MFM) was utilized (Scheme S1, ESI†). The MFM images and corresponding AFM images are shown in Fig. 2. We examined whether the nanohybrids possessed the magnetic property or not by analyzing phase difference in each image. As can be seen in Fig. 2(d), the titania/ODA/Fe(acac)$_3$ nanohybrids exhibited a clear contrast during the MFM observation, indicating that the nanohybrids possess the magnetic property. On the other hand, almost no contrast was observed in the MFM image of the titania/ODA nanohybrids when the contrast range was set at the same as that in the case of the titania/ODA/Fe(acac)$_3$ nanohybrids. Thus, we decreased the contrast range to obtain the clearer image, although the image is still unclear (Fig. 2(b)), indicating almost no magnetic property. For more detailed characterizations, the vibrating sample magnetometer (VSM) curves of these two samples were also measured. As shown in Fig. 2(e), the slight magnetization was observed in response to the applied magnetic field in the case of the titania/ODA/Fe(acac)$_3$ nanohybrids, while titania/ODA nanohybrids did not show an apparent response. Judging from these results, the titania/ODA/Fe(acac)$_3$ nanohybrids possess a paramagnetic property. Since the paramagnetic behavior should be affected by the amount of Fe(acac)$_3$ incorporated into the titania matrix, we are now trying to control molar Fe/Ti ratio of the titania/ODA/Fe(acac)$_3$ nanohybrids.

A color of titania-based materials is known as an important indicator for various applications. In the present case, the titania/ODA/Fe(acac)$_3$ powder sample looked slightly yellowish, which is due to the presence of Fe(acac)$_3$ molecules. Thus, the diffuse reflectance UV-Vis spectra were measured to discuss an optical property of the nanohybrids. Fig. S6 in ESI† indicates that the titania/ODA/Fe(acac)$_3$ nanohybrids have two characteristic absorption bands: a large absorption band in the UV range and a relatively small absorption band in the visible range. Band gap energies of these bands could be 3.1 eV (approx. 400 nm) and 2.4 eV (approx. 520 nm), respectively. To attribute an origin of each absorption band, the photoexcitation and photoluminescence spectra were also measured. Fig. S7 in ESI† demonstrates the excitation and luminescence spectra of the titania/ODA and titania/ODA/Fe(acac)$_3$ nanohybrids in powder and IPA dispersion states. In both cases, a clear luminescence peak was observed at around 459 nm when the samples were excited by excitation wavelength of 421 nm, suggesting that the large absorption band can be assigned to titania itself. The excitation and luminescence spectra of Fe(acac)$_3$ shown in Fig. S8 in ESI† exhibit intense peaks at around 518 nm and 610 nm, respectively. Thus, the small absorption in the visible range seen in Fig. S6† is probably due to Fe(acac)$_3$ incorporated into the titania/ODA/Fe(acac)$_3$ nanohybrids.

One of the most interesting phenomena discovered in the present study is that the titania/ODA/Fe(acac)$_3$ nanohybrids demonstrated clear luminescence at approx. 600 nm with the excitation wavelength of approx. 535 nm (Fig. 3) while both pristine titania and Fe(acac)$_3$ did not show luminescence. The reason for this unexpected luminescence can be explained on the basis of Fe(acac)$_3$ concentration in the nanohybrids. In the case of pristine Fe(acac)$_3$ dissolved in IPA, the luminescence intensity decreases when the concentration of Fe(acac)$_3$ increases from 6 mM to 22 mM where the Fe(acac)$_3$ concentration in the solution A is almost in this range (Fig. S8(b), ESI†). This result implies that the luminescence quenching occurs in this concentration range. Taking into account that the concentration of Fe(acac)$_3$ molecules in the titania/ODA/Fe(acac)$_3$ nanohybrids is estimated to be 1.34×10^{-18} mol per particle (Fig. S9, ESI†),[28] a possible reason for the clear

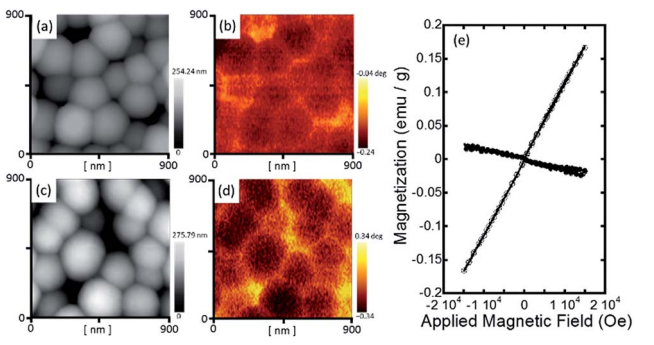

Fig. 2 (a and c) AFM and (b and d) MFM images of the (a and b) titania/ODA and (c and d) titania/ODA/Fe(acac)$_3$ nanohybrids, and (e) VSM curves of titania/ODA (closed circles) and titania/ODA/Fe(acac)$_3$ (open circles) nanohybrids.

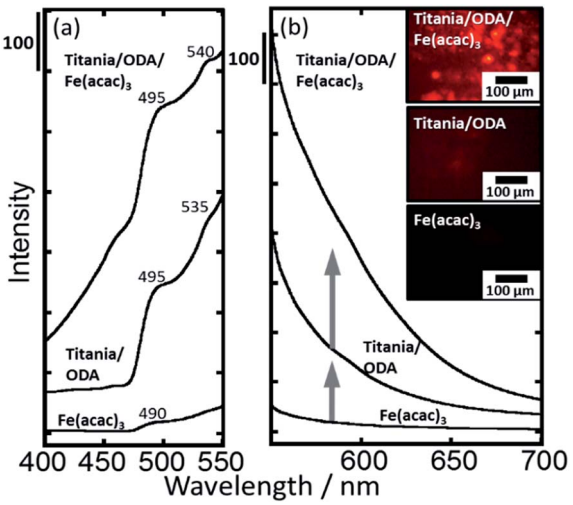

Fig. 3 (a) Excitation and (b) luminescence spectra of the nanohybrids and neat Fe(acac)$_3$ powder (inset in (b): the fluorescent microscope images).

luminescence can be understood because this concentration is out of the quenching range mentioned above. For more detailed discussion, the distance between the incorporated $Fe(acac)_3$ molecules was estimated through a simple geometrical calculation. As a result, the distance was 1.0 nm, indicating that no cross relaxation and/or excitation migration occurs in this case. In contrast, no luminescence was observed in the case of $Fe(acac)_3$ powder apparently because of the quenching effect. Thus, $Fe(acac)_3$ would be incorporated into the nanohybrids without significant aggregation that induces luminescence quenching.

For the detailed understanding of the interesting luminescence property, a formation mechanism and resultant nanostructure of the titania/ODA/$Fe(acac)_3$ nanohybrids have to be considered. A proposed formation mechanism of the present nanohybrids is shown in Fig. 4. Previous reports pointed out that an acetylacetone interacts with a titanium alkoxide.[21,22] Specifically, oxygen atoms in the acetylacetone structure interact with a central Ti atom in the alkoxide structure to form a stable chelating compound as we also discussed with the IR results (Fig. S2, ESI†). This chelating reaction can proceed with the molar ratio of alkoxide : acetylacetone up to 1 : 1, which is rather high value as compared with the present case, 1 : 0.02. Since the starting solution looked transparent and homogeneous even after adding $Fe(acac)_3$ into TTIP/IPA mixture, it is possible to say that $Fe(acac)_3$ molecules are dissolved in the form of Ti–$Fe(acac)_3$ chelating compounds. Thus, the chelating compounds should be uniformly distributed in the TTIP/IPA solution, realizing the proper $Fe(acac)_3$–$Fe(acac)_3$ distance that triggered the enhanced luminescence. Another study reported that the nucleation of titania occurred in the presence of $Fe(acac)_3$.[29] In the previous report, the hydrolysis of TTIP was conducted by mixing a TTIP/IPA solution with an aqueous IPA solution containing $Fe(acac)_3$, leading to the formation of uniform nuclei with the size of approx. 3 nm which is consistent with that reported in our previous studies.[3,24] Two surface OH groups of a titania nucleus are thought to react with one $Fe(acac)_3$ to generate one chelating compound and two acetylacetone molecules. Taking account of these results, following reaction mechanism can be proposed: reaction of TTIP with $Fe(acac)_3$ in the starting solution to form the Ti-chelating compounds, and hydrolysis and condensation reaction of the chelating compounds in the microfluidic channel to form the uniform sized nuclei. Based on the IR results shown in Fig. S2,† $Fe(acac)_3$ interacts both with surface OH groups and Ti–O–Ti. Therefore, $Fe(acac)_3$ should be present both on titania surface and inside titania structure. Taking into account that estimated distance between $Fe(acac)_3$ molecules is approx. 1.0 nm, a larger number of $Fe(acac)_3$ molecules are present on the titania surface because the size of titania nuclei is 2–3 nm. After the microfluidic reaction processes, the nuclei are added into an aqueous IPA solution containing ODA, resulting in the formation of monodispersed spherical nanohybrids composed of the nuclei *via* self-assembly driven by hydrophobic interaction even though the nuclei contain hetero-atoms or molecules.[3,20,30,31] Since the $Fe(acac)_3$ species would be homogeneously distributed in/on the titania nuclei, luminescence quenching was suppressed. Therefore, the titania/ODA/$Fe(acac)_3$ nanohybrids demonstrated the enhanced luminescence property.

In summary, monodispersed titania/ODA hybrid spherical nanohybrids containing $Fe(acac)_3$ were successfully synthesized by the homogeneous nucleation of the titania-based hybrid in a microfluidic channel and subsequent growth in a reaction container. The nanohybrids exhibited a paramagnetic behavior which is due to the incorporated $Fe(acac)_3$. Furthermore, the nanohybrids demonstrated an enhanced luminescence property. Since the incorporated $Fe(acac)_3$ molecules were homogeneously distributed in the nanohybrids without aggregation and segregation, the efficient luminescence was realized. Taking advantage of the present approach utilizing a metal acetylacetonate as a precursor, various metallic species can be incorporated into titania matrix to obtain well-defined titania-based hybrid nanomaterials with unique functionalities, allowing for such applications as the luminescent pigments, visible light-driven photocatalysts, and bio-imaging with chemo, photo, magneto-therapy.

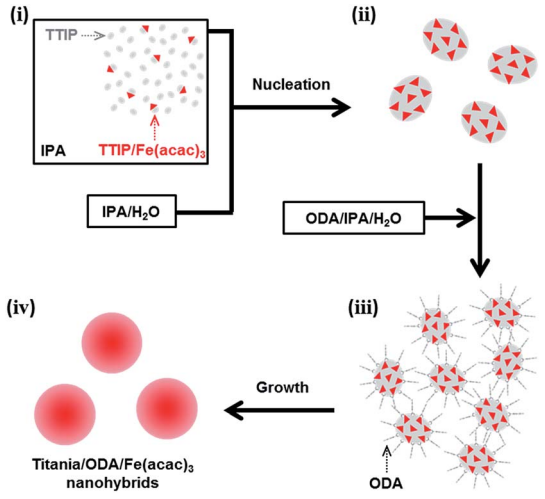

Fig. 4 Illustration for the proposed formation mechanism of titania/ODA/$Fe(acac)_3$ nanohybrids.

Acknowledgements

This research was supported by the World Premier International Research Center Initiative on Materials Nanoarchitectonics (WPI-MANA); the Grant-in-Aid for Young Scientists (B) 26870836, MEXT/JSPS KAKENHI, Japan; the Grant-in-Aid for Young Scientists (A) 26709052, MEXT/JSPS KAKENHI, Japan.

Notes and references

1 J. Kim, O. Wilhelm and S. E. Pratsinis, *J. Am. Ceram. Soc.*, 2001, **84**, 2802.
2 A. S. Deshpande, D. G. Shchukin, E. Ustinovich, M. Antonietti and R. A. Caruso, *Adv. Funct. Mater.*, 2005, **15**, 239.
3 K. Shiba and M. Ogawa, *J. Ceram. Soc. Jpn.*, 2011, **119**, 507.

4 J. Yan, X. Li, S. Cheng, Y. Ke and X. Liang, *Chem. Commun.*, 2009, 2929.
5 J. Yu, L. Yue, S. Liu, B. Huang and X. Zhang, *J. Colloid Interface Sci.*, 2009, **334**, 58.
6 H. Fei, Y. Liu, Y. Li, P. Sun, Z. Yuan, B. Li, D. Ding and T. Chen, *Microporous Mesoporous Mater.*, 2007, **102**, 318.
7 X. S. Li, G. E. Fryxell, M. H. Engelhard and C. Wang, *Inorg. Chem. Commun.*, 2007, **10**, 639.
8 H. Xu, Z. Zheng, L. Zhang, H. Zhang and F. Deng, *J. Solid State Chem.*, 2008, **181**, 2516.
9 S. K. Das, S. Darmakolla and A. J. Bhattacharyya, *J. Mater. Chem.*, 2010, **20**, 1600.
10 F.-F. Cao, X.-L. Wu, S. Xin, Y.-G. Guo and L.-J. Wan, *J. Phys. Chem. C*, 2010, **114**, 10308.
11 L. Li, C. K. Tsung, Z. Yang, G. D. Stucky, L. D. Sun, J. F. Wang and C. H. Yan, *Adv. Mater.*, 2008, **20**, 903.
12 J. Yin, L. Xiang and X. Zhao, *Appl. Phys. Lett.*, 2007, **90**, 113112.
13 H. Li, G. Liu, S. Chen and Q. Liu, *Phys. E*, 2010, **42**, 1844.
14 J. Li, J. Xu, W.-L. Dai, H. Li and K. Fan, *Appl. Catal., B*, 2009, **85**, 162.
15 H.-G. Jung, C. S. Yoon, J. Prakash and Y.-K. Sun, *J. Phys. Chem. C*, 2009, **113**, 21258.
16 W. Ho, J. C. Yu and S. Lee, *Chem. Commun.*, 2006, 1115.
17 J. H. Pan, Z. Cai, Y. Yu and X. S. Zhao, *J. Mater. Chem.*, 2011, **21**, 11430.
18 B. Chi, L. Zhao and T. Jin, *J. Phys. Chem. C*, 2007, **111**, 6189.
19 K. M. Parida and B. Naik, *J. Colloid Interface Sci.*, 2009, **333**, 269.
20 K. Shiba, S. Sato and M. Ogawa, *J. Mater. Chem.*, 2012, **22**, 9963.
21 A. Yamamoto and S. Kambara, *J. Am. Chem. Soc.*, 1957, **79**, 4344.
22 A. Yamamoto and S. Kambara, *J. Am. Chem. Soc.*, 1959, **81**, 2663.
23 K. Shiba and M. Ogawa, *Chem. Commun.*, 2009, 6851.
24 K. Shiba, K. Onaka and M. Ogawa, *RSC Adv.*, 2012, **2**, 1343.
25 Q. Jin, M. Fujishima and H. Tada, *J. Phys. Chem. C*, 2011, **115**, 6478.
26 I. Georgieva, N. Danchova, S. Gutzov and N. Trendafilova, *J. Mol. Model.*, 2011, **18**, 2409.
27 B. Pal and M. Sharon, *Thin Solid Films*, 2000, **379**, 83.
28 This value was calculated based on average particle size, collected amount of the hybrid from the starting solution and molar Fe/Ti ratio. See Fig. S9 in ESI† for details.
29 S. Tieng, R. Azouani, K. Chhor and A. Kanaev, *J. Phys. Chem. C*, 2011, **115**, 5244.
30 K. Shiba, M. Tagaya, T. Sugiyama and N. Hanagata, *RSC Adv.*, 2015, **5**, 104343.
31 K. Shiba, M. Tagaya and N. Hanagata, *ACS Appl. Mater. Interfaces*, 2014, **6**, 6825.